


Article

Dependence of the Atomic Structure of Solid Solutions in the Pd-Cu System Ordered According to the B2 Type on the Composition

Valentin M. Ievlev ^{1,2,*}, Konstantin A. Solntsev ², Alexander L. Vasiliev ^{3,4}, Semen V. Gorbunov ², Alexey I. Dontsov ⁵ , Nataliya R. Roshan ², Sergey V. Kannykin ⁵, Alexey V. Ovcharov ⁶ and Bugakov V. Alexander ⁷

¹ Department of Material Science, Moscow State University, 119991 Moscow, Russia

² Baikov Institute of Metallurgy and Materials Science, Russian Academy of Sciences, 119334 Moscow, Russia

³ Institute of Crystallography, Russian Academy of Sciences, 119333 Moscow, Russia

⁴ Moscow Institute of Physics and Technology, 141701 Moscow, Russia

⁵ Department of Materials Science and Nanosystems Industry, Voronezh State University, 394018 Voronezh, Russia

⁶ National Research Centre “Kurchatov Institute”, 123098 Moscow, Russia

⁷ Faculty of Radio Engineering and Electronics, Voronezh State Technical University, 394000 Voronezh, Russia

* Correspondence: rnileme@mail.ru



Citation: Ievlev, V.M.; Solntsev, K.A.; Vasiliev, A.L.; Gorbunov, S.V.; Dontsov, A.I.; Roshan, N.R.; Kannykin, S.V.; Ovcharov, A.V.; Alexander, B.V. Dependence of the Atomic Structure of Solid Solutions in the Pd-Cu System Ordered According to the B2 Type on the Composition. *Processes* **2022**, *10*, 2632. <https://doi.org/10.3390/pr10122632>

Academic Editor: Song Hu

Received: 7 November 2022

Accepted: 28 November 2022

Published: 7 December 2022

Publisher’s Note: MDPI stays neutral with regard to jurisdictional claims in published maps and institutional affiliations.



Copyright: © 2022 by the authors. Licensee MDPI, Basel, Switzerland. This article is an open access article distributed under the terms and conditions of the Creative Commons Attribution (CC BY) license (<https://creativecommons.org/licenses/by/4.0/>).

Abstract: Owing to exceptionally high selectivity, membranes based on palladium alloys are widely used for obtaining high-purity hydrogen. An important issue for providing high hydrogen permeability of the membranes is to form the required phase composition. The structural organization of the solid solutions consisting of Cu–36.4 at. % Pd and Cu–50 at. % Pd were studied by X-ray diffraction (XRD), electron diffraction (ED), high-resolution transmission electron microscopy (HRTEM) and energy dispersive X-ray spectroscopy (EDXS). It was found that the former composition can be ordered in the temperature range of 300–400 °C and in the heating (up to 800 °C)–cooling cycle. In the presence of excess Cu atoms (27.2%), this structure can be represented by CsCl type structural units (β -phase) and distributed body center cubic (BCC) copper structural units in the corresponding concentration dose. The formation of a single crystal ordered phase within the mosaic blocks of the disordered phase was established. Experimental evidence was obtained for the separation of the α -phase solid solution in the elemental composition; the very low rate of ordering inherent in this system was attributed to this effect. The hydrogen permeability of a foil of the equiatomic composition was described.

Keywords: solid solution; Pd–Cu system; ordering; structure; hydrogen permeability

1. Introduction

The main trends of modern energy engineering are energy conservation and transition to environmentally safe technologies. Therefore, considerable attention is paid to renewable energy sources such as solar and wind energy, and so on [1]. In order to ensure uninterrupted power supply, it is necessary to use these sources with energy storage devices, including those based on hydrogen cycle [2,3]. Hydrogen exists in nature only in the bound state, and is mainly produced by coal gasification and steam reforming of methane [4,5]. However, only high-purity hydrogen is applicable for the most common types of fuel cells based on proton exchange membranes, for microelectronics, and for some other applications [6]. The most promising hydrogen purification process is based on the use of highly selective membranes based on palladium alloys [7]; the capacity of this process depends on the phase composition of the membranes. This brings about the interest in solid solutions in the Pd–Cu system corresponding to the state diagram region [8] in which B2 type ordering takes place to give the CsCl type structure (β -phase). Several-fold lower activation energy

for hydrogen diffusion in the β -phase than in palladium [9] is responsible for the high productivity of the membrane. In addition, the use of these systems makes it possible to avoid the formation of hydrides and, hence, to eliminate dilation characteristic of pure or doped palladium [10]. The economic expediency of manufacturing membranes based on this system in comparison with membranes based on doped palladium is also significant.

The ordering and disordering (transfer to the face centered cubic (FCC) α -phase) processes are being vigorously studied for various compositions of solid solutions [10–12]. An extremely low rate of ordering was found in the vicinity of the equiatomic composition [13]. The nature of the decrease in the $\alpha \rightarrow \beta$ transformation rate has not yet been discussed. The necessity of deviation of the composition from the equiatomic ratio towards increasing copper content was demonstrated to be a necessary condition for β -phase generation [14]. The deformation effect during ordering was established [15,16]. It was found that the phase composition and texture of the Pd-Cu alloy formed in successive steps of foil rolling are controlled by the transformation mechanism [17].

An X-ray diffraction study of the $\beta \leftrightarrow \alpha$ transformation in a hydrogen medium showed that the β -phase boundary shifts towards higher temperatures by 150–200 °C [18,19].

It was found that rapid photon treatment by xenon lamp irradiation (0.2–1.2 μm spectrum) leads to pronounced acceleration of disordering and α -phase stabilization [20,21]; this enables comparison of the mechanical properties of foils of the same elemental composition with β and α phase structures.

The substructure of two-phase films is studied at the submicrometer level by transmission electron microscopy (TEM) [13,16]; however, there is still a lack of experimental data on the structural organization of α and β phases at the nano-scale level. Meanwhile, these data are needed for the understanding of the nature of observed effects and substantiation of the practically important properties of B2-ordered systems. In particular, for the system in question, it is necessary to interpret the concentration dependence of the ordering rate and the increase in the electrical resistivity upon disorder.

The present study is aimed at gaining data on the structural organization of a single-phase foil of an ordered Pd-Cu solid solution at high deviation from the equiatomic composition towards increasing copper content (up to the β -phase boundary at 500 °C [8]) using the potential of X-ray diffraction (XRD) and high-resolution transmission electron microscopy (HRTEM) techniques. Another goal is to interpret the decrease in the $\alpha \rightarrow \beta$ phase transition rate for a near-equiatomic composition by considering the necessary condition of β -phase nucleation [14].

2. Materials and Methods

Pd-Cu foils containing 36.4 at. %Pd (Cu-Pd36), approximately 30 μm thick, and 50 at. %Pd (Cu-Pd50), approximately 18 μm thick.

The alloys were prepared by arc melting in an inert gas atmosphere (purified argon or helium) using nonconsumable tungsten electrode and water-cold copper bottom. Studied foils 18, 30 μm in thickness were prepared in accordance with the following manufacturing scheme:

Ingots \rightarrow Rolling with a vacuum mill \rightarrow Rolling with four-roll mill \rightarrow Rolling with twenty-roll mill.

The rolling with four- and twenty-roll mills were performed using intermediate annealings.

Ordering and disordering processes were studied in situ by X-ray diffraction on an ARL X'TRA diffractometer (Thermo Fisher Scientific, Waltham, MA, USA) and by resistometry (Installation for measuring surface resistance, Russia) using heating–cooling cycles. The relative orientation and substructure of adjacent α - and β -phases were studied by electron diffraction, HRTEM, and energy-dispersive X-ray (EDX) microanalysis on an Osiris (Thermo Fisher Scientific, USA) transmission electron microscope at an accelerating voltage of 200 kV. The instrument was equipped with a high-angle annular dark-field (HAADF) detector (Fischione, Pittsburgh, PA, USA) and a Super X EDXS (ChemiSTEM, Bruker, Billerica, MA, USA). The images were processed using the Digital Micrograph

(Gatan, Pleasanton, CA, USA) and the TIA (Thermo Fisher Scientific, USA) software. The samples for electron microscopy examination and microanalysis were prepared using a focused Ga⁺ ion beam in a Helios Nano Lab 600 i dual-beam scanning electron ion microscope (Thermo Fisher Scientific, USA) at an accelerating voltage of 30 kV in initial stages and 2 kV in final stages. Hydrogen permeability was measured on the original stand by filling a calibrated volume using a high-temperature working cell in which the membrane was placed. The setup includes a cell with the mounted palladium-alloy membrane, which is placed into an electric furnace and heated to a working temperature. Working gasses (from standard vessels) are fed to the cell through a pipeline system. The amount of pure hydrogen separated with the membrane is measured with a “SAPFIR” unit intended for measuring low discharges (hydrogen is burned off with flame). The rate of gas flow passed thorough the membrane is determined (with the “SAPFIRE”) using the inleakage time for a calibrated volume that was preliminarily evacuated to a residual pressure of 0.02 MPa. A portion of pure hydrogen is analyzed with a chromatograph that also is used to analyze the hydrogen-depleted gas mixture (it is also burned off with flame). The pressures of starting gas mixture and pure hydrogen is determined with manovacuummeters. Temperatures of the body, internal volume and membrane are measured with chromel-alumel thermocouple and continuously are recorded with a multipoint KSP-4 potentiometer.

3. Results

The initial Cu-Pd36 foil sample comprises two phases and has nanocrystalline structure, with a low proportion of the β -phase, which forms a $\langle 100 \rangle$ texture characteristic of the Nishiyama–Wasserman orientation relationship [22,23]. Figure 1 shows the X-ray diffraction patterns of the Cu-Pd36 sample during heating to 800 °C (1–8) and cooling to room temperature (9–15).

Table 1 characterizes the change in the phase composition and the crystal lattice parameter of the phases. The ordering is activated by high deformation during rolling.

Table 1. Variation of the phase composition and crystal lattice parameters (a , Å) of the phases during the heating–cooling cycle of the Cu-Pd36 sample.

T, °C	Heating		Cooling	
	α -Phase	β -Phase	α -Phase	β -Phase
25	3.7440(9)	2.936(2)	3.7385(9)	2.9647(4)
200	3.746(1)	2.9641(5)	3.7334(1)	2.9579(1)
300	-	2.9708(2)	3.746(1)	2.9682(5)
400	-	2.9745(3)	3.7551(2)	2.9729(5)
500	3.7549(7)	2.9799(3)	3.7549(2)	2.979(2)
600	3.7651(6)	-	3.761(2)	-
700	3.7729(6)	-	3.7700(8)	-
800	3.7817(6)	-		

During heating of the initial Cu-Pd36 sample to 800 °C, complete ordering is attained in the temperature range of 300–400 °C (X-ray diffraction patterns 2 and 3 in Figure 1a). This is consistent with the reported data [17], indicating that the subsequent heat treatment of the Cu-Pd36 foil at 300 °C leads to complete ordering of the structure. After heating up to 800 °C, the foil recrystallizes and complete ordering does not take place during the subsequent cooling (X-ray diffraction pattern 15).

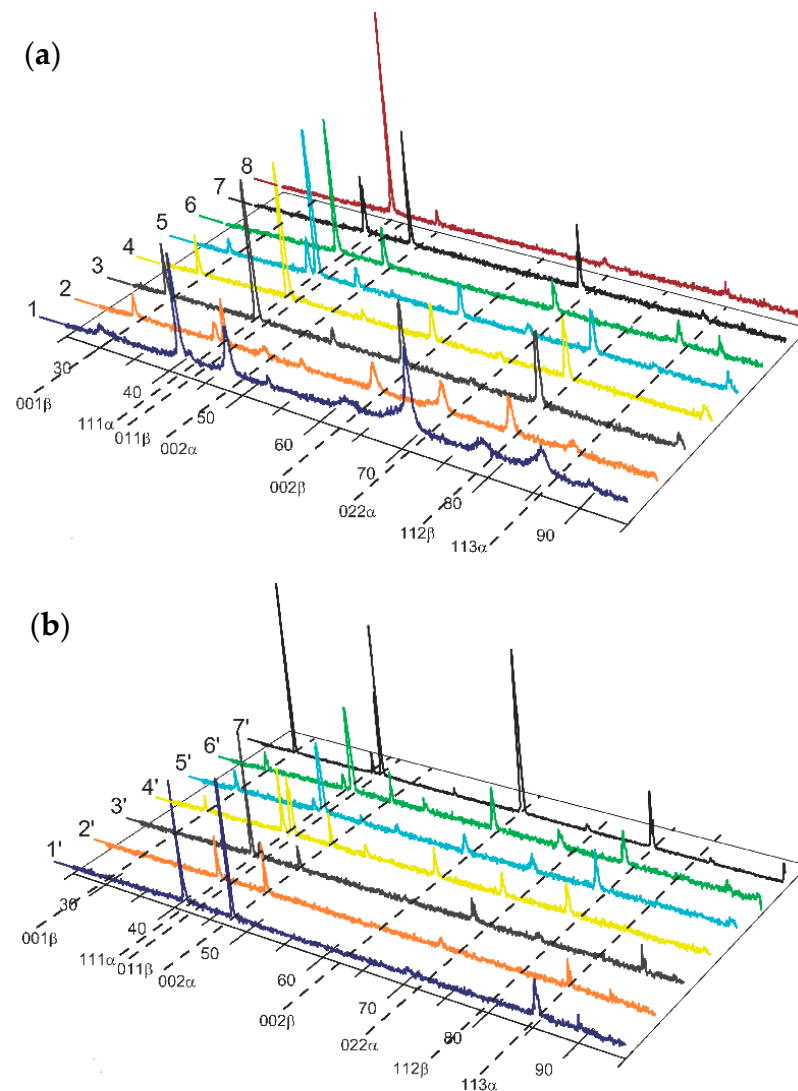


Figure 1. Variation of the X-ray diffraction patterns of the Cu-Pd36 sample during: (a) heating up to 25 (1), 200 (2), 300 (3), 400 (4), 500 (5), 600 (6), 700 (7), and 800 °C (8); (b) cooling down to 700 (1'), 600 (2'), 500 (3'), 400 (4'), 300 (5'), 200 (6'), and 25 °C (7').

The completely “ordered” atomic structure detected by X-ray diffraction with excess Cu atoms (27.2%) can be interpreted as being formed by CsCl type-based structural units and BCC-based Cu units elastically accommodated to them in a proportion corresponding to excess Cu atoms. The absence of additional reflections provides experimental evidence for this atomic structure: the structural factor for the BCC Cu basis and β -phase basis pre-determines the superimposition of all reflections of the BCC structure on the corresponding reflections of the CsCl type structure.

This structure can be considered as a limiting case of bulk pseudomorphism, analogue of surface pseudomorphism on epitaxy (for example, the formation of BCT Cu atomic layers on the (001) Pd surface [24,25]).

The mutual accommodation of structural units upon the formation of this “ordered” solid solution structure is manifested as a smaller crystal lattice parameter compared to the lattice parameter of the completely ordered near-equiatom structure; for example, for the Cu-49 at. %Pd system, $a\beta = 2.978$ Å [26]; for the Cu-43 at. %Pd system, $a\beta = 2.972$ Å; and for the system studied here, $a\beta = 2.9579$ Å [27]. This indicates that the proportion of BCC Cu structural units corresponding to the initial elemental composition is retained in all stages of the $\beta \leftrightarrow \alpha$ transformations in two-phase structures.

Incomplete ordering of the Cu-Pd36 foil as a result of the heating–cooling cycle enables studying the features of structural nucleation of the ordered phase within the initial α -phase. Figure 2 shows the selected area electron diffraction (SAED) pattern of a thin section of the two-phase sample after the heating–cooling cycle. It follows from the SAED pattern that the orientation relationship between the β - and α -phases is close to the Nishiyama–Wasserman relationship.

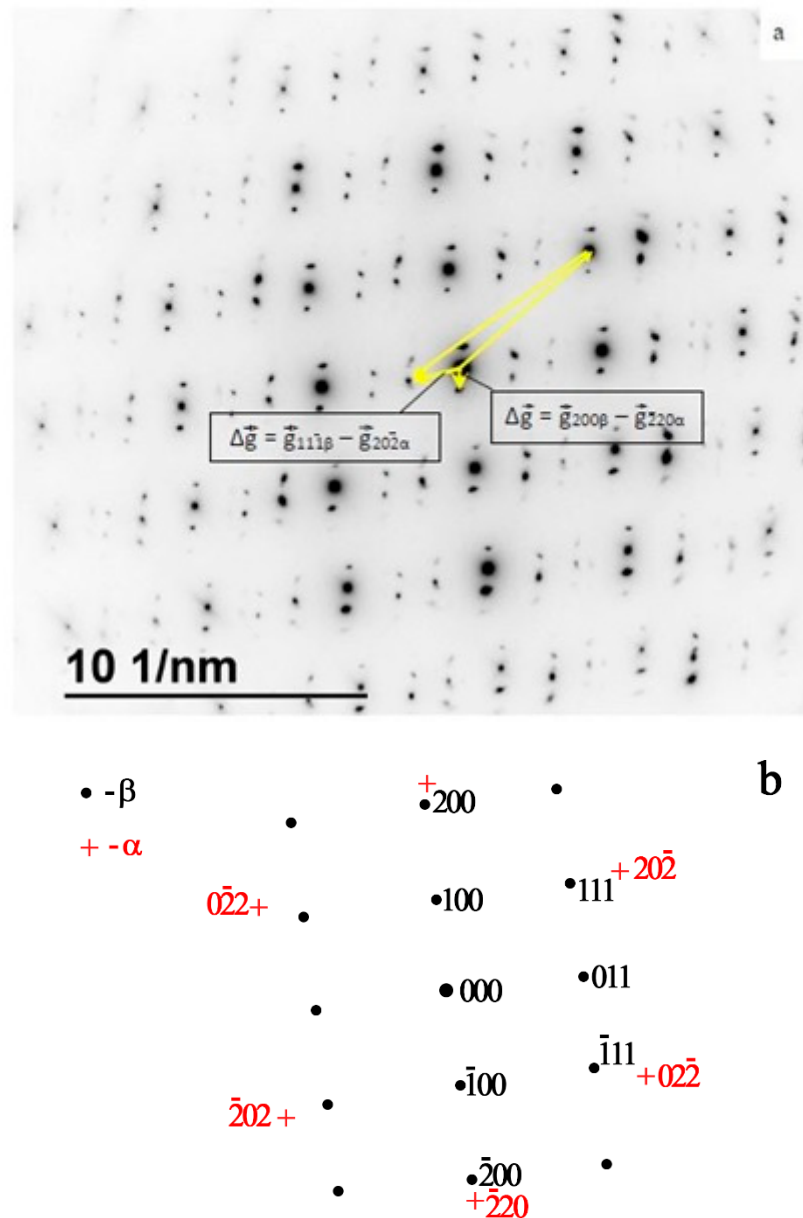


Figure 2. (a) SAED pattern of a section of two-phase Cu-Pd36 sample and (b) its interpretation: (1) β -phase reflections, (2) α -phase reflections; the other reflections are due to double diffraction. The highlighted vectors correspond to the interference bands in Sections 1 and 2.

The β -phase predominates, and diffuse reflections of the α -phase with sharp point reflections of the β -phase provides the conclusion that the single crystal β -phase is formed within a studied area of the initial phase with the mosaic substructure. This conclusion is also confirmed by HRTEM image (Figure 3).

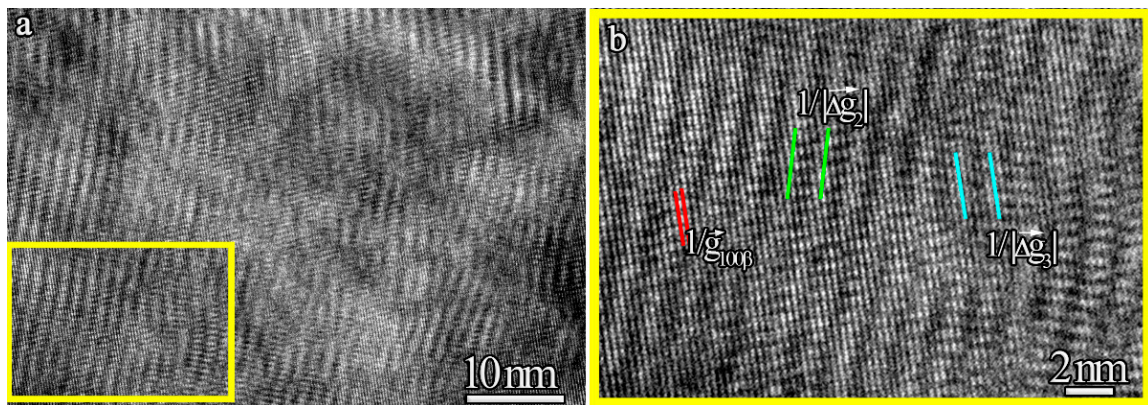


Figure 3. (a) HRTEM image of a part of the Cu-Pd36 sample within the block of α -phase subgrains, (b) enlarged fragment containing interference bands with a period equal to the β -phase crystal lattice parameter $\frac{1}{|\vec{g}_{100\beta}|}$, and moiré patterns with the periods $\frac{1}{|\Delta\vec{g}_2|}$ and $\frac{1}{|\Delta\vec{g}_3|}$ (2 and 3).

While there are strictly periodic interference lines (interference of the 000 and 100 β beams) with the period $\frac{1}{|\vec{g}_{100}|}$ (\vec{g} is the reflection vector from index planes) corresponding to the β -phase structure parameters, breaks of moiré patterns with the periods $PM1 = \frac{1}{|\vec{g}_{200\beta} - \vec{g}_{220\alpha}|}$ and $PM2 = \frac{1}{|\vec{g}_{111\beta} - \vec{g}_{220\alpha}|}$ are observed as a result of double diffraction within the overlapping β -phase sections and adjacent α -phase subgrains.

The formation of the single crystal ordered structure is due to the multiple discrete nucleation of the β -phase and subsequent coalescence, which takes place on going across the small-angle α -phase subgrain boundaries. The nature of limiting nanocluster organization illustrates the EDXS element distribution maps (Figure 4). The size of Cu clusters is in the range between 0.5 and 1.5 nm.

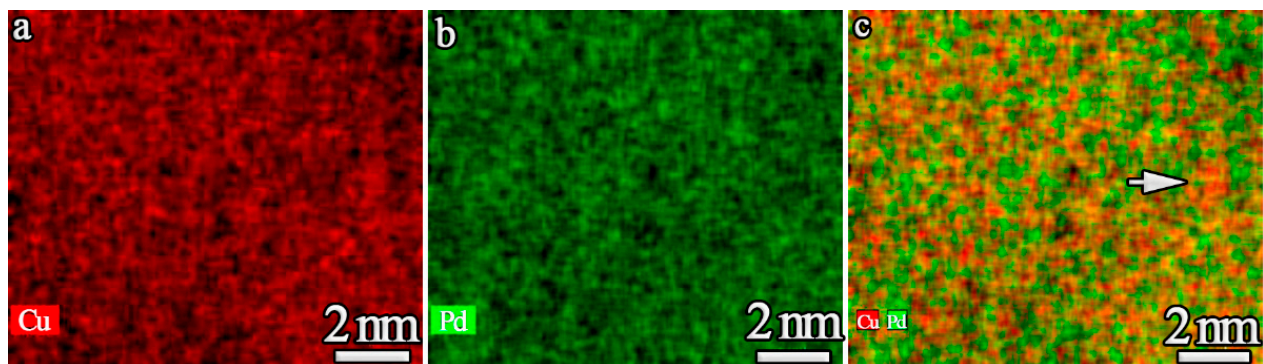


Figure 4. Distribution of components (EDXS element maps) in the Cu-Pd36 sample: (a) Cu, (b) Pd, (c) Cu + Pd. One of Cu cluster is indicated by an arrow.

The molecular dynamic study of hydrogen atom diffusion in the thin Pd foil model [28] showed the retention of hydrogen atoms in structure defects. Therefore, hydrogen atoms are expected to be retained by the local deviations from the β -phase structure distributed in the “ordered” structure.

The Cu-Pd50 sample also has a $\langle 110 \rangle_\alpha$ texture; the heat treatment gives a recrystallized microstructure with a crystal lattice parameter (3.7440(9) Å) corresponding to the specified elemental composition of the α -phase [8]. Figure 5 shows the X-ray diffraction patterns of the Cu-Pd50 sample for the cycle including heating to 800 °C and cooling to room temperature.

Figure 6a,b demonstrate Cu and Pt distribution of α -phase components, respectively obtained by EDXS mapping. It follows that this structure contains approximately an order of magnitude larger clusters than the ordered structure of the Cu-Pd36 sample.

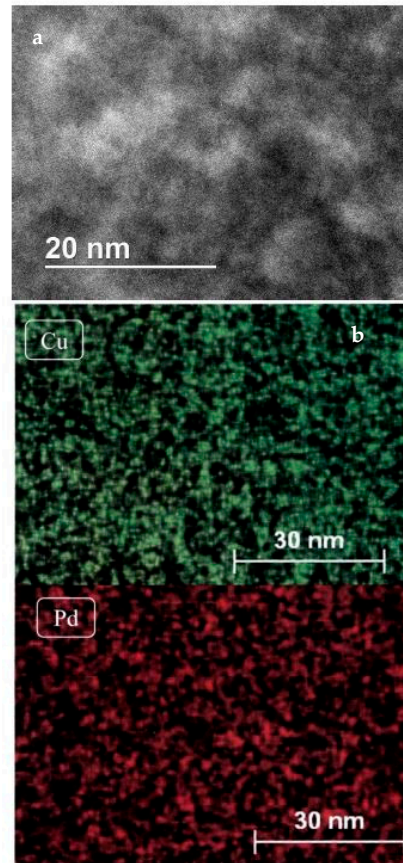


Figure 6. EDXS elemental mapping of the Cu-Pd50 specimen: (a) Cu and (b) Pd. The Cu cluster is indicated by an arrow.

Figure 7 characterizes the variation of the electrical resistivity in the heating (1)–cooling (2) cycle.

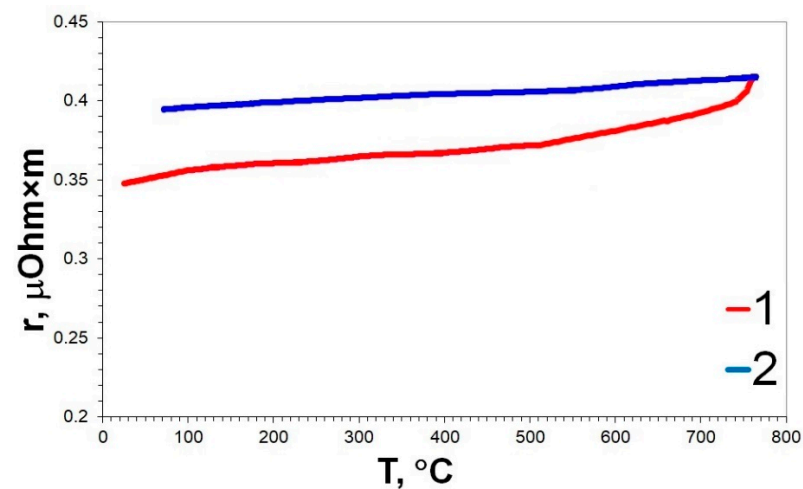


Figure 7. Temperature dependence of the electrical resistivity of the Cu-Pd50 foil in the heating (1)–cooling cycle (2).

These data are correlated with the X-ray diffraction data (Figure 5): the heating of the initial sample in the vicinity of 300 °C and 400 °C gives rise to weak inflections towards increasing electrical resistivity characterizing the “attempt” at system ordering (the X-ray diffraction pattern shows weak β -phase reflections in this region) activated by the preliminary deformation during rolling. After cooling from 800 °C, the single-phase recrystallized structure (α -phase) is retained. During the subsequent heat treatment (300 °C, 4 h), the phase composition does not change. These results characterize the exceptionally low rate of ordering of the equiatomic Cu-Pd system, which is in line with conclusions of previous studies [10–13].

The effect of elemental composition on the rate of ordering can be interpreted considering the obvious statement that a uniform equiatomic solid solution of a two-component system with an infinite mutual solubility is always ordered. In the case of a disordered system (in this case, α -phase), “phase separation” in the elemental composition inevitably takes place to give a nanocluster crystal structure with a mutual cluster accommodation, resulting in an averaged crystal lattice parameter. In this structure, the probability of β -phase nucleation, i.e., the formation of structural units composed of palladium atoms surrounded by 8 copper atoms [14], is low.

The decrease in the electrical conductivity characteristic of two-component solid solutions occurs for near-equiatomic compositions [29], which can be attributed to electron scattering at cluster boundaries (the limiting case of the classical size effect of electrical conductivity [30]). The phase separation of this type can also account for low hydrogen permeability of the near-equiatomic disordered Pd-Cu structure: the hydrogen atoms are retained at the phase boundary like at a grain boundary [28].

Figure 8 characterizes the time dependence of hydrogen permeability of the Cu-Pd50 foil at 320 °C.

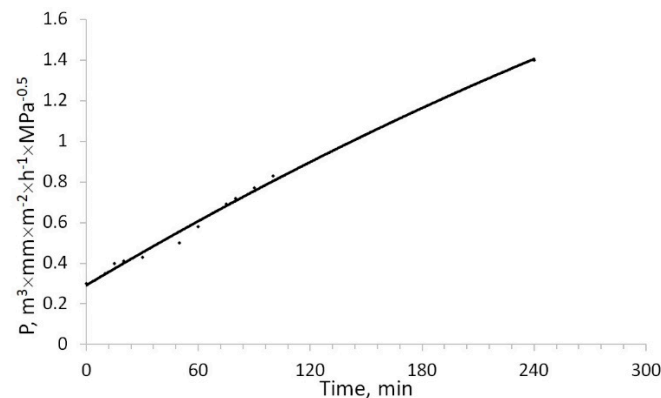


Figure 8. Time dependence of the hydrogen permeability (Q , $(\text{m}^3 \cdot \text{mm})/(\text{m}^2 \cdot \text{h} \cdot \text{MPa}^{0.5})$) of a Cu-Pd50 membrane foil sample at 320 °C.

The fourfold increase in the hydrogen permeability for approximately 6 h is caused by foil recrystallization (α -phase), resulting in crystallite growth and decrease in the fraction of interfaces retarding hydrogen transfer. In this case, hydrogen permeability of the foil reaches the level characteristic of best membranes of palladium alloys [31].

4. Conclusions

The discrete nucleation of the β -phase and the subsequent coalescence of the nuclei result in the formation of a single crystal ordered structure within the block of α -phase subgrains.

Complete “ordering” of the solid solution with limiting deviation from the equiatomic composition towards increasing copper content gives rise to a nanocluster atomic structure composed of CsCl and BCC Cu structural units present in the amounts predetermined by the elemental composition. The phase separation of the equiatomic solid solution and the

formation of a nanocluster single-phase structure (α -phase) was confirmed experimentally; this forms the basis for interpretation of the low rate of $\alpha \rightarrow \beta$ transformation.

Author Contributions: V.M.I.—formal analysis and writing an article; K.A.S.—review writing and editing; A.L.V.—study of the orientation and substructure of adjacent phases α and β on a foil of a given composition; S.V.G.—investigation of the properties of the permeability of a foil of a given composition; A.I.D.—study of the processes of ordering and disordering of a foil of a given composition; N.R.R.—obtaining foil samples of a given composition; S.V.K.—study of samples by X-ray diffractometry; A.V.O.—preparation of samples for research by electron microscopy and microanalysis; B.V.A.—processing of the obtained results. All authors have read and agreed to the published version of the manuscript.

Funding: The work is carried out within the framework of the state assignment No. 75-00328-22-00.

Data Availability Statement: Not applicable.

Acknowledgments: Academician of the Russian Academy of Sciences Yaroslavl'tsev A.B. for help at work.

Conflicts of Interest: The authors declare no conflict of interest.

References

- Pagliaro, M.; Meneguzzo, F. Digital management of solar energy en route to energy self-sufficiency. *Glob. Chall.* **2019**, *3*, 1800105. [CrossRef]
- Song, J.; Wei, C.; Huang, Z.-F.; Liu, C.; Zeng, L.; Wang, X.; Xu, Z.J. A review on fundamentals for designing oxygen evolution electrocatalysts. *Chem. Soc. Rev.* **2020**, *49*, 2196–2214. [CrossRef] [PubMed]
- Filippov, S.P.; Yaroslavl'tsev, A.B. Hydrogen energy: Development prospects and materials. *Russ. Chem. Rev.* **2021**, *90*, 627–643. [CrossRef]
- Verma, A.; Olateju, B.; Kumar, A.; Gupta, R. Development of a process simulation model for energy analysis of hydrogen production from underground coal gasification (UCG). *Int. J. Hydrogen Energy* **2015**, *40*, 10705–10719. [CrossRef]
- Chen, L.; Qi, Z.; Zhang, S.; Su, J.; Somorjai, G.A. Catalytic Hydrogen Production from Methane: A Review on Recent Progress and Prospect. *Catalysts* **2020**, *10*, 858. [CrossRef]
- Abe, J.O.; Popoola, A.P.I.; Ajenifuja, E.; Popoola, O.M. Hydrogen energy, economy and storage: Review and recommendation. *Int. J. Hydrogen Energy* **2019**, *44*, 15072–15086. [CrossRef]
- Basile, A. Hydrogen production using pd-based membrane reactors for fuel cells. *Top. Catal.* **2008**, *51*, 107. [CrossRef]
- Subramanian, P.R.; Laughlin, D.E. Cu-Pd (Copper-Palladium). *J. Phase Equilib.* **1991**, *12*, 231–243. [CrossRef]
- Alefeld, G. Hydrogen in metals. (Topics in applied physics; v. 28–29). Includes Bibliographical References and Indexes. Contents: V. 1. Basic properties. v. 2. Application-oriented properties. 1. Metals-Hydrogen Content. 1. 1933, I1. V61kl, J., 1936-TH690.H97. Available online: <https://vdoc.pub/documents/hydrogen-in-metals-i-basic-properties-2gd1gnngum70> (accessed on 5 November 2022).
- Shiraishi, T. Ordering Process in CuPd Alloys during Continuous Heating. *J. Jpn. Inst. Met.* **1982**, *46*, 245–252. [CrossRef]
- Novikova, O.S.; Antonova, O.V.; Volkov, A.Y. Formation of an ordered structure in the Cu–50 at % Pd alloy. *Phys. Met. Metallogr.* **2021**, *122*, 651–656. [CrossRef]
- Volkov, A.Y.; Novikova, O.S.; Antonov, B.D. The kinetics of ordering in an equiatomic CuPd alloy: A resistometric study. *J. Alloys Compd.* **2013**, *581*, 625–631. [CrossRef]
- Ievlev, K.M.; Solntsev, K.A.; Dontsov, A.I.; Belonogov, E.K.; Kannykin, S.V. phase transformations in rolled foil of the Pd-57 at % Cu solid solution. *Inorg. Mater.* **2017**, *53*, 1163–1169. [CrossRef]
- Volkov, A.Y.; Kruglikov, N.A. Effect of plastic deformation on the kinetics of phase transformations in the Cu-47Pd alloy. *Phys. Met. Metallogr.* **2008**, *105*, 202–210. [CrossRef]
- Novikova, O.S.; Volkova, E.G.; Glukhov, A.V.; Antonova, O.V.; Kostina, A.E.; Antonov, B.D.; Volkov, A.Y. Evolution of the microstructure, electrical resistivity and microhardness during atomic ordering of cryogenically deformed Cu-47 at.% Pd alloy. *J. Alloys Compd.* **2020**, *838*, 155591. [CrossRef]
- Levlev, V.M.; Dontsov, A.I.; Gorbunov, S.V.; Il'inova, T.N.; Kannykin, S.V.; Prizhimov, A.S.; Roshan, N.R.; Solntsev, K.A. Structure, Texture, and Substructure of Foil in Sequential Rolling Steps of Cu-36.4 at % Pd Alloy. *Inorg. Mater.* **2021**, *57*, 1194–1200.
- Opalka, S.M.; Huang, W.; Wang, D.; Flanagan, T.B.; Lovvik, O.M.; Emerson, S.C.; She, Y.; Vanderspurt, T. Hydrogen interactions with the PdCu ordered B2 alloy. *J. Alloys Compd.* **2007**, *446–447*, 583–587. [CrossRef]
- Levlev, V.M.; Solntsev, K.A.; Dontsov, A.I.; Maksimenko, A.A.; Kannykin, S.V. Hydrogen Permeability of Thin Condensed Pd-Cu Foil: Dependence on Temperature and Phase Composition. *Tech. Phys.* **2016**, *61*, 467–469.
- Levlev, V.M.; Solntsev, K.A.; Serbin, O.V.; Dontsov, A.I.; Sinetskaya, D.A.; Roshan, N.R. The Effect of Rapid Photon Treatment of the PdCu Solid Solution Foil of Near-Equiatomic Composition. *Dokl. Chem.* **2019**, *489 Pt 1*, 275–277. [CrossRef]

20. Ievlev, V.M.; Dontsov, A.I.; Prizhimov, A.S.; Serbin, O.V.; Roshan, N.R.; Gorbunov, S.V.; Sinetskaya, D.A.; Solntsev, K.A. Flash Lamp Processing-Activated Structural Transformations in Foil of a Pd-Cu Solid Solution. *Inorg. Mater.* **2020**, *56*, 577–582. [[CrossRef](#)]
21. Burkhanov, G.S.; Gorina, N.B.; Kolchugina, N.B.; Roshan, N.R.; Slovetkii, D.I.; Chistov, E.M. Palladium-based alloy membranes for separation of high-purity hydrogen from hydrogen-containing gas mixtures. *Platinum Metals Rev.* **2011**, *55*, 3–12. [[CrossRef](#)]
22. Nishiyama, Z. X-ray Investigation of the Mechanism of the Transformation from Face-Centered Cubic Lattice to Body-Centered Cubic. *Sci. Rep. Tohoku Imp. Univ.* **1934**, *23*, 637–664.
23. Wasserman, G. Influence of the α - γ -Transformation of an Irreversible Ni Steel onto Crystal Orientation and Tensile Strength. *Arch. Eisenhüttenwes.* **1933**, *45*, 145–170.
24. Li, H.; Wu, S.C.; Tian, D.; Quinny, Y.; Li, Y.S.; Yona, F. Epitaxial growth of body-centered-tetragonal copper. *Phys. Rev. B* **1989**, *40*, 5841–5844. [[CrossRef](#)]
25. Elmar, H.; Elisabeth, K.; Nicolas, W.; Klaus, K. Strain driven fcc-bct phase transition of pseudomorphic Cu films on Pd (100). *Phys. Rev. Lett.* **1995**, *74*, 1803–1806.
26. Volkov, A.Y.; Novikova, O.S.; Antonov, B.D. Formation of an ordered structure in the CU–49 AT % PD alloy. *Inorg. Mater.* **2012**, *48*, 1262. [[CrossRef](#)]
27. Ievlev, V.M.; Dontsov, A.I.; Maksimenko, A.A.; Roshan, N.R. reversibility of the $\beta \rightleftharpoons \alpha$ phase transformations in a PD–CU solid solution. *Inorg. Mater.* **2017**, *53*, 484–488. [[CrossRef](#)]
28. Ievlev, V.M.; Prizhimov, A.S.; Boldyreva, A.V. Interaction of hydrogen atoms with grain boundaries in palladium bicrystals. *Inorg. Mater.* **2018**, *54*, 421–425. [[CrossRef](#)]
29. Gottstein, G. *Physical Foundations of Materials Science*; Springer: Berlin/Heidelberg, Germany, 2004; p. 400.
30. Larson, D.C. *Physics of Thin Films*; Francombe, M.H., Hoffman, R.W., Eds.; Academic Press: New York, NY, USA, 1971; Volume 6, p. 81.
31. Ievlev, V.M.; Prizhimov, A.S.; Dontsov, A.I. Structure of the α – β interface in a PdCu solid solution. *Phys. Solid State* **2020**, *62*, 59–64. [[CrossRef](#)]